Liquid Crystals
Publication details, including instructions for authors and subscription information:
http://www.informaworld.com/smpp/title~content=t713926090

A homologous series of chiral swallow-tailed materials possessing an antiferroelectric phase with V-shaped switching property

S. -L. Wu; P. -L. Chang

To cite this Article Wu, S. -L. and Chang, P. -L.(2002) 'A homologous series of chiral swallow-tailed materials possessing an antiferroelectric phase with V-shaped switching property', Liquid Crystals, 29: 10, 1355 — 1359

To link to this Article: DOI: 10.1080/713935616

URL: http://dx.doi.org/10.1080/713935616

LIQUID CRYSTALS, 2002, VOL. 29, NO. 10, 1355–1359

Taylor & Francis
Taylor & Francis Group

A homologous series of chiral swallow-tailed materials possessing an antiferroelectric phase with V-shaped switching property

S.-L. WU* and P.-L. CHANG
Department of Chemical Engineering, Tatung University,
40 Chungshan N Rd 3rd Sec., Taipei 104, Taiwan, ROC

(*Received 5 May 2002; accepted 8 July 2002*)

A homologous series of chiral swallow-tailed materials, 1-ethylpropyl (*S*)-2-{6-[4-(4′-alkoxyphenyl)benzoyloxy]-2-naphthyl}propionates EP*m*PBNP (*m* = 8–14), was prepared for investigating the effect of non-chiral alkyl chain length on the electro-optical response of the antiferroelectric phase. With the exception of EP8PBNP which shows monotropic SmC^*_A phase, the materials show an enantiotropic phase sequence of $\mathrm{BP}_{\mathrm{II}}$–N*–TGBA*–SmA*–$\mathrm{SmC}^*_A$. The maximum spontaneous polarization measured for these materials in the antiferroelectric phase were in the approximate range 20–30 $\mathrm{nC\,cm^{-2}}$, indicating that the materials possess low polarity. The electro-optic responses measured for the materials in polyimide film-coated homogeneously aligned cells, displayed a thresholdless V-shaped switching property. Our results clearly demonstrate that the non-chiral alkyl chain lengths have no effect on the appearance of V-shaped switching in antiferroelectric phase, but that the applied frequency and cell thickness significantly affect switching behaviours.

1. Introduction

Thresholdless, V-shaped switching in chiral smectic liquid crystals [1] has become a very attractive subject for both academic scientists and technical engineers because this type of material is very promising for display applications [2]. Investigations on chiral materials based on the Inui and Mitsui mixtures that showed V-shaped switching have been extended [1–14], and several structural models [1, 2, 13, 14] have been proposed to account for the essential molecular structure at the tip of the V-shape, and the dynamic phenomenon of the V-switching. The reported results indicate that V-shaped switching behaviour strongly depends on the alignment films, films thickness, cell gap and applied frequency. Although the importance of substrate surface interactions between alignment film and liquid crystal has been emphasized, the role of the molecular structure of liquid crystals on switching behaviour has not yet been fully explored.

We recently reported a novel chiral swallow-tailed material, EP10PBNP, that shows antiferroelectricity with V-shaped switching in a polyimide-coated homogeneous cell [15]. In consequence, a homologous series of structurally similar materials has been prepared for a first attempt at investigating the effect of molecular structure on the electro-optical response of the antiferroelectric phase. The general structural formula of the chiral swallow-tailed materials, 1-ethylpropyl (*S*)-2-{6-[4-(4′-alkoxyphenyl)benzoyloxy]-2-naphthyl}-propionates, EP*m*PBNP (*m* = 8–14), is depicted below.

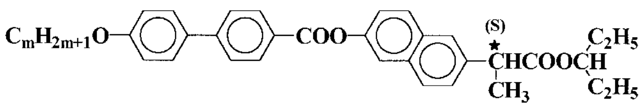

2. Experimental

2.1. *Characterization of materials*

The chemical structures for the target materials were identified by proton nuclear magnetic resonance (^{1}H NMR) spectroscopy using a JEOL EX-400 FT-NMR spectrometer. The purity of the final compounds was assessed by thin layer chromatography (TLC), and further confirmed by elemental analysis using a Perkin-Elmer 2400 instrument. The analytical data showed that the percentage errors for the carbon and hydrogen contents for the target materials were less than 1% as compared with the calculated results. The transition temperatures and enthalpies for all materials were determined by differential scanning calorimetry (DSC) using a Perkin-Elmer DSC7 calorimeter at a rate of 5°C $\mathrm{min^{-1}}$. Mesophases were identified by microscopic textures using a Nikon Microphot-FXA optical microscope under crossed polarizers with an INSTEC HS1 hot stage in connection with a RTC heat controller. Sample cells were purchased from E. H. C. Co., Japan. The cells, with 0.25 $\mathrm{cm^2}$ conducting area, were fabricated with a coating of unidirectionally buffed polyimide film. Switching

---

*Author for correspondence; e-mail: slwu@ttu.edu.tw

Liquid Crystals ISSN 0267-8292 print/ISSN 1366-5855 online
http://www.tandf.co.uk/journals
DOI: 10.1080/02678290210000029453

behaviour and electro-optical response of the antiferroelectric smectic phase were investigated by the triangular wave method [16].

2.2. *Preparation of materials*

The synthetic procedures were carried out in the same manner as described previously [17] and are shown in the scheme. The starting chiral material for the synthesis of compounds EP*m*PBNP was (*S*)-2-(6-methoxy-2-naphthyl)propionic acid, purchased from Tokyo Chemical Industry (TCI) Co. Ltd, Japan, with optical purity greater than 99% enantiomeric excess. Tetrahydrofuran (THF) and dichloromethane (CH_2Cl_2), were dried by treating with $LiAlH_4$ and CaH_2, respectively, and distilled before use. The acid **1** was esterified with 1-ethylpropanol in the presence of DCC and DMAP to produce the esters 1-ethylpropyl (*S*)-2-(6-methoxy-2-naphthyl)-propionates **2**. The methoxy group of these esters was demethylated by treatment with BBr_3, and the resulting hydroxy group of 1-ethylpropyl (*S*)-2-(6-hydroxy-2-naphthyl)propionate **3** was subsequently esterified with a variety of 4-(4′-alkoxyphenyl)benzoic acids **4** ($m = 8$–14) using DCC and DMAP, to produce the target materials EP*m*PBNP. ^{1}H NMR data and elemental analysis for the target materials are in accord with expected results.

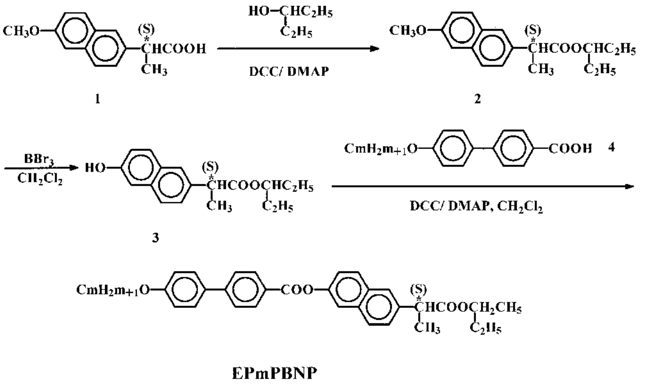

Scheme.

3. Results and discussion

3.1. *Mesomorphic properties*

The mesophases were principally identified by microscopic texture observations. The appearance of the $\mathrm{BP_{II}}$ phase was characterized by a non-iridescent platelet texture. The N* phase was identified by the appearance of scale-like or fan-like textures. A TGBA* intermediate between N* and SmA* phases, was characterized by the appearance of a spiral filament texture [18, 19]. This phase displayed a Grandjean-like texture with steps between twist states varying by half the pitch [20] in the 5 µm thickness of homogeneously polyimide coated cells. The SmA* phase was identified by the appearance of a focal-conic and homeotropic texture. The antiferroelectric SmC_A^* phase appeared as a striated focal-conic texture, with an apparently helical pitch band in the thicker sample region and a schlieren texture with two- and four-brush singularities [21, 22] in the thinner sample region. The appearance of a strip-shaped domain along the smectic layer normal in the 2 µm thickness of homogeneous cells, and the alternation of bright and dark stripes on applying an electric field, further support the assignment of the SmC_A^* phase [23].

Table. Transition temperature and enthalpies ΔH (in italics) of materials EP*m*PBNP at 5°C min^{-1} scanning rate. Cr = crystal, m.p. = melting point, [] denotes a monotropic transition.

	T/°C and ΔH/J g^{-1} (in italics)													
m		I		$\mathrm{BP_{II}}$		N*		TGBA*		SmA*		SmC_A^*	Cr	m.p.
8	•	156.1	•	155.0^a	•	142.7	•	141.0^a	•	[93.0]^b	•	[83.9]	•	101.1
		1.2				*1.6*						*53.0*		*61.6*
9	•	146.2	•	145.4^a	•	131.3	•	130.9^a	•	98.3	•	69.6	•	97.8
		1.3				*0.7*				*0.2*		*37.3*		*44.8*
10	•	143.1	•	134.4^a	•	129.0^a	•	128.2^a	•	102.5	•	54.2	•	84.2
		6.7								*0.4*		*28.3*		*36.5*
11	•	138.8	•	132.3^a	•	128.6	•	126.2^a	•	102.1	•	51.5	•	78.4
		1.2				*0.7*				*0.2*		*25.6*		*28.3*
12	•	139.6	•	138.8^a	•	131.3	•	129.6^a	•	110.3	•	56.4	•	90.4
		1.8				*0.6*				*0.4*		*64.2*		*78.2*
13	•	133.0	•	132.8^a	•	127.0	•	125.8^a	•	106.4	•	54.9	•	80.2
		1.6				*0.7*				*0.2*		*61.7*		*67.0*
14	•	135.7	•	135.4^a	•	130.4	•	129.6^a	•	110.9	•	64.7	•	90.7
		2.7				*1.1*				*0.3*		*80.2*		*81.4*

[a] The enthalpies of $\mathrm{BP_{II}}$–N* or TGBA*–SmA* transitions were added together with that of the I–$\mathrm{BP_{II}}$ transition or N*–TGBA*.

[b] The enthalpy was too small to be measured.

Mesophases and their corresponding phase transition temperatures obtained by DSC on cooling are given in the table. With the exception of EP8PBNP which shows a monotropic $S_{C_A}^*$ phase, all of the materials reveal an enantiotropic phase sequence: BP_{II}–N*–TGBA*–SmA*–SmC_A^*. The results indicate that the BP_{II} phase is comparatively more stable at $m=10$ and $m=11$. The thermal stability of the SmA* phase decreases, while that of the SmC_A^* phase increases, as m ascends.

3.2. *Physical properties*

Materials sandwiched separately in 2 and 5 μm homogeneous cells were used for the measurement of physical properties in the antiferroelectric phase. Spontaneous polarization ($\mathbf{P}_s$) values, measured as a function of temperature for all materials on cooling, are presented in figure 1. The $\mathbf{P}_s$ values gradually increase as the temperature decreases and reach maximum values of approximate 20–30 nC cm^{-2}. It is worth pointing out that these materials display two frustrated phases: BP_{II} and TGBA*, indicating that the materials have high chirality [24]. However, the measured maximum $\mathbf{P}_s$ values are significantly lower than that reported earlier by us for some structurally similar chiral materials where a straight chain or methyl-substituted alkyl group was attached at the chiral part of the molecules [25, 26]. It is considered that the decreasing $\mathbf{P}_s$ values might be due to the influence of increasing excluded volume by the swallow-tailed group at the chiral tail of the molecules. Our previous result showed that the electro-optical response of EP10PBNP exhibited V-shaped switching, suggesting that this switching behaviour can be achieved in an antiferroelectric liquid crystal with low polarization. It is worth noting that the components in the Inui and Mitsui mixtures are generally derived from a homologous series of chiral tail groups with a highly polar trifluoromethyl substituent attached to the chiral centre. Consequently, the mixtures possesed high polarization, the maximum value for Inui mixture being about 170 nC cm^{-2} [13].

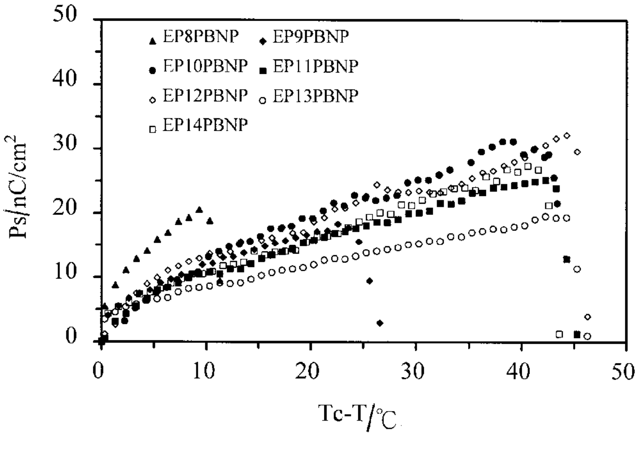

Figure 1. Spontaneous polarization $\mathbf{P}_s$ plotted as a function of temperature for the materials EPmPBNP ($m=9$–14). T_c is the SmA*–SmC_A^* transition temperature.

In order to investigate the effect of peripheral alkyl chain length on the electro-optical response in the antiferroelectric phase, measurements were conducted by

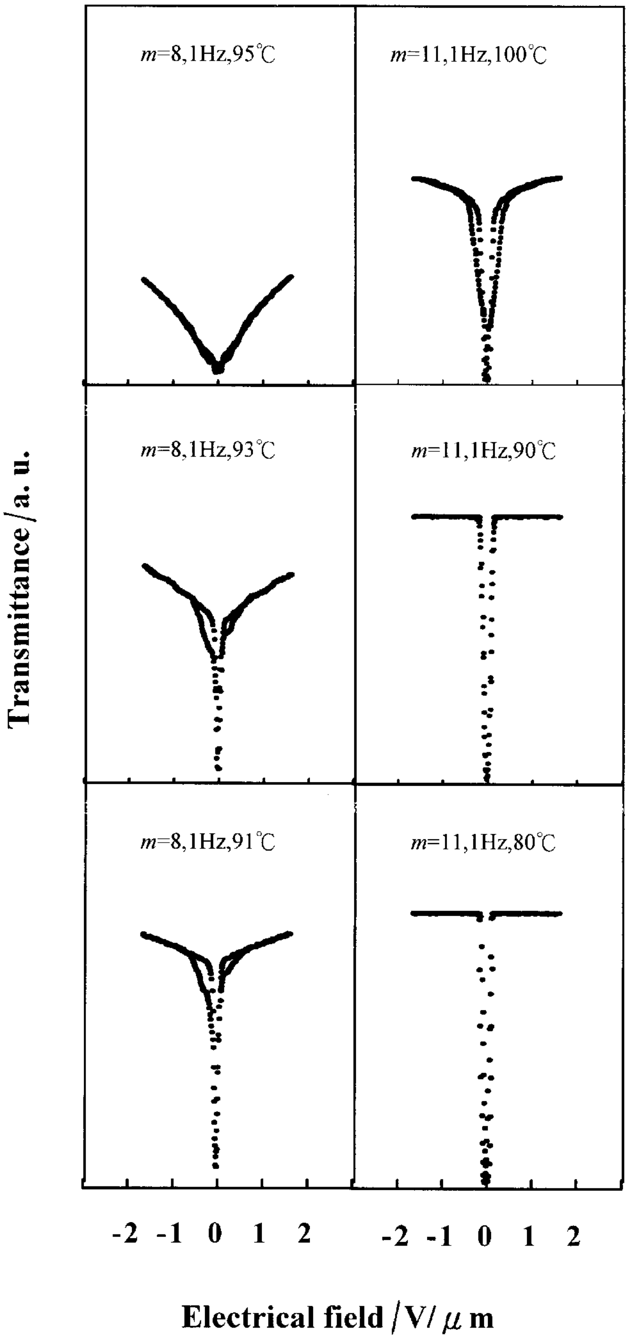

Figure 2. Optical transmittance as a function of applied electric field for the materials EP8PBNP and EP11PBNP in 5 μm homogeneous cells at various temperatures; measured by applying a triangular waveform at 1 Hz frequency.

using 5 μm homogeneous cells and applying a triangular waveform at 1 Hz frequency. Some representative results for the responses of optical transmittance versus electric field measured on EP*m*PBNP compounds are presented in figures 2, 3 and 4. It is seen, in general, that the responses critically depend on temperature: as the temperature decreases, the maximum transmittance values increase. This phenomenon has been proposed as due to the increase of the tilt angle [7]. In the case of EP*m*PBNP ($m = 8$ and 9), the responses display slight hysteresis and a ferrielectric-like switching behaviour [6] throughout the temperature range of the antiferroelectric

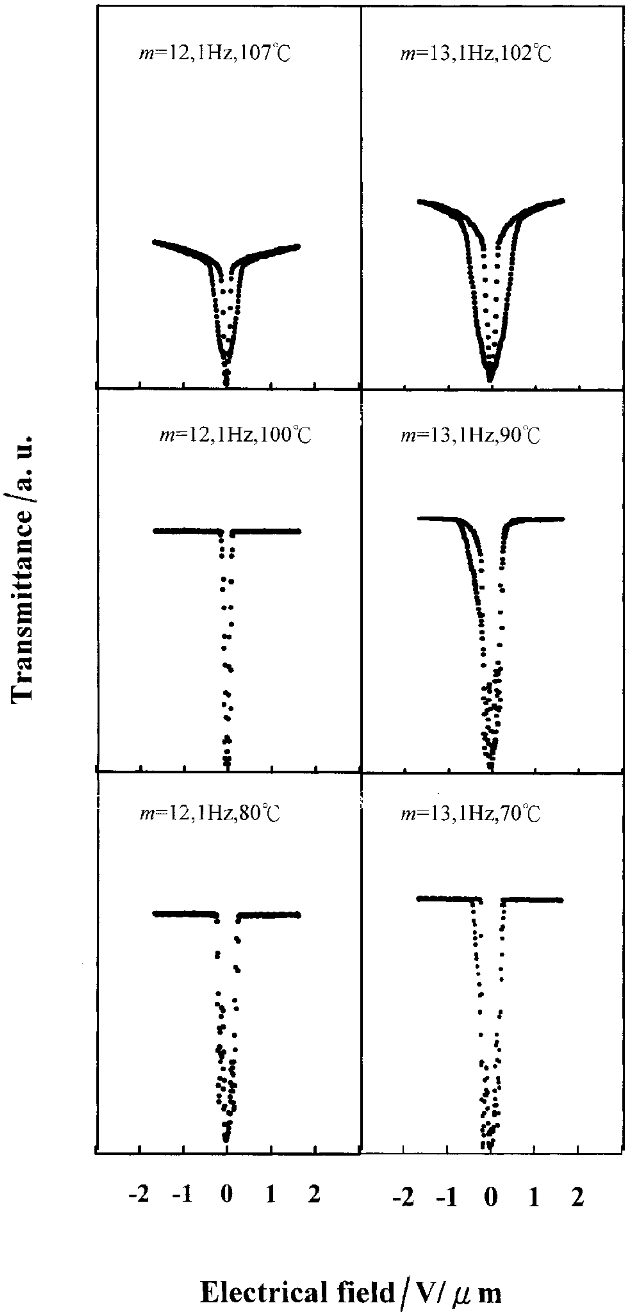

Figure 3. Optical transmittance as a function of applied electric field for the materials EP12PBNP and EP13PBNP in 5 μm homogeneous cells at various temperatures; measured by applying a triangular waveform at 1 Hz frequency.

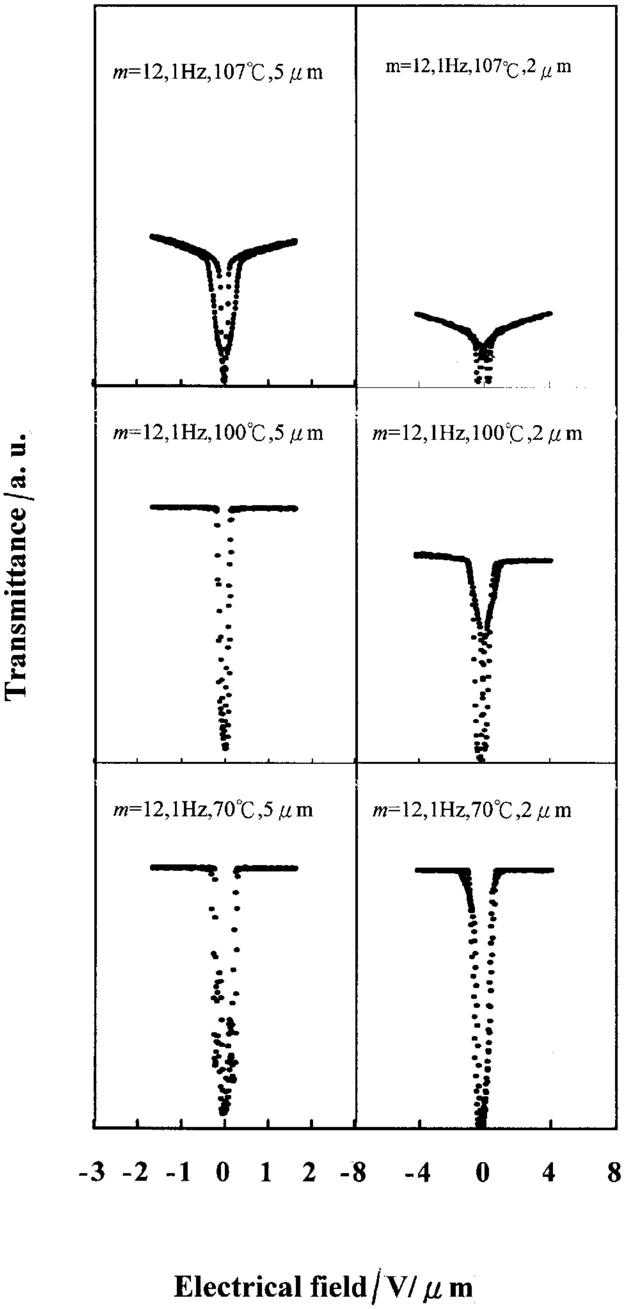

Figure 4. Optical transmittance as a function of applied electric field for the material EP12PBNP in 5 μm and 2 μm homogeneous cells at various temperatures; measured by applying a triangular waveform at 1 Hz frequency.

phase, as shown in a typical example for EP8PBNP in figure 2. However, in the case of EP*m*PBNP ($m = 10$ and 11), the ferrielectric-like switching behaviour appears only when the temperature changes immediately from SmA* phase to antiferroelectric phase. On further lowering of the temperature, V-shaped swiching occurs and remains unchanged until the material crystallizes, as shown in a typical example for EP11PBNP in figure 2. When the alkyl chain lengths increase to $m = 12$, the electro-optical response shows a ferrielectric-like switching at a temperature near the SmA*–SmC$_A^*$ transition, and then alters to V-shaped switching. But as the temperature decreases below 107°C, as shown in figure 3, the tip of the V-shape becomes distorted. This kind of distorted switching behaviour also occurs as the alkyl chain length increases to $m = 13$ and 14, as shown in a typical example for EP13PBN in figure 3. This phenomenon, however, was corrected when the materials were measured in 2 μm cells; V-shaped switching appears, as shown in figure 4 at 70°C, though it is altered to W-shaped switching at 100°C. This clearly indicates that the V-shaped switching behaviour critically depends on the thickness of the homogeneous cell.

4. Conclusions

A homologous series of chiral swallow-tailed materials, derived from (*S*)-2-(6-hydroxy-2-naphthyl)propionic acid, possess antiferroelectric SmC$_A^*$ phases with the property of V-shaped switching. Our results indicate that these chiral materials of low polarity can achieve thresholdless, V-shaped switching in the antiferroelectric phase. Moreover, this optical switching behaviour is not affected by variation of the non-chiral alkyl chain, but significantly depends on the temperature of the phase, applied frequency and cell thickness.

This work was supported by the National Science Council of the R.O.C. through Grant No. NSC-89-2215-E036-001.

References

[1] Inui, S., Limura, N., Suruki, T., Iwane, H., Miyachi, F., Takanishi, Y., and Fukuda, A., 1996, *J. mater. Chem.*, **6,** 671.

[2] Saishu, T., Takatih, K., Iida, R., Nagata, H., and Mori, Y., 1996, *SID'96 Dig.*, **28,** 4.

[3] Fukuda, A., Seomun, S. S., Takanashi, T., Takanishi, Y., and Ishikawa, K., 1997, *Mol. Cryst. liq. Cryst.*, **303,** 379.

[4] Seomun, S. S., Takanashi, T., Ishikawa, K., Takezoe, H., Fukuda, A., Tanaka, C., Fujiama, T., Maruyama, T., and Nishiyama, S., 1997, *Mol. Cryst. liq. Cryst.*, **303,** 181.

[5] Seomun, S. S., Takanashi, Y., Ishikawa, K., Takezoe, H., and Fukuda, A., 1997, *Jpn. J. appl. Phys.*, **36,** 3586.

[6] Seomun, S. S., Park, B., Chandani, A. D. L., Herman, D. S., Takanashi, Y., Ishikawa, K., Takezoe, H., and Fukuda, A., 1998, *Jpn. J. appl. Phys.*, **37,** L698.

[7] Seomun, S. S., Gouda, T., Takanashi, Y., Ishikawa, K., Takezoe, H., and Fukuda, A., 1999, *Liq. Cryst.*, **26,** 167.

[8] Chandani, A. D. L., Cui, Y., Seomun, S. S., Takanishi, Y., Ishikawa, K., Takezoe, H., and Fukuda, A., 1999, *Liq. Cryst.*, **26,** 167.

[9] Park, B., Nakata, M., Seomun, S. S., Takanishi, Y., Ishikawa, K., and Takezoe, H., 1999, *Jpn. J. appl. Phys.*, **38,** 1474.

[10] Park, B., Nakata, M., Seomun, S. S., Takanishi, Y., Ishikawa, K., and Takezoe, H., 1999, *Phys. Rev. E*, **59,** R3815.

[11] Matsumoto, T., Fukuda, A., Johno, M., Motoyama, Y., Yui, T., Seomun, S. S., and Yamashita, M., 1999, *J. mater. Chem.*, **9,** 2051.

[12] Takeuchi, M., Ke, C., Ando, T., Matsumoto, T., Fukuda, A., and Yamashita, M., 2000, *Ferroelectrics*, **246,** 1.

[13] Rudquist, R., Lagerwall, J. P. F., Buivydas, M., Gouda, F., Lagerwall, S. T., Clark, N. A., Maclennan, J. E., Shoa, R., Coleman, D. A., Bardon, S., Bellini, T., Link, D. R., Natale, G., Glaser, N. A., Walba, D. M., Wand, M. D., and Chen, X.-H., 1999, *Chem. Mater.*, **9,** 1257.

[14] Clark, N. A., Coleman, D., and Maclennan, J. E., 2000, *Liq. Cryst.*, **27,** 985.

[15] Wu, S.-L., and Hsieh, W.-J., 1999, *J. mater. Chem.*, **11,** 852.

[16] Miyasato, K., Abe, S., Takazoe, H., Fukuda, A., and Kuze, T., 1983, *Jpn. J. appl. Phys.*, **22,** L661.

[17] Wu, S.-L., Yen, P. C., and Hsieh, W.-J., 1998, *Liq. Cryst.*, **24,** 741.

[18] Wu, S.-L., and Hsieh, W.-J., 1996, *Liq. Cryst.*, **21,** 783.

[19] Kuczynski, W., and Sfegemeyer, H., 1994, *Ber. Bunsenges. Phys. Chem.*, **98,** 1322.

[20] Dierking, I., and Lagerwall, S. T., 1999, *Liq. Cryst.*, **21,** 783.

[21] Takanishi, Y., Takezoe, H., Fukuda, A., Komura, H., and Watanabe, H., 1992, *J. mater. Chem.*, **2,** 71.

[22] Gisse, P., Pavel, J., Nguyen, H. T., and Lorman, V. L., 1993, *Ferroelectrics*, **147,** 27.

[23] Suzuki, Y., Hagiwara, T., Kawamura, I., Okamura, N., Kitazume, T., Kakimoto, M., Imai, Y., Ouchi, Y., Takezoe, H., and Fukuda, A., *Liq. Cryst.*, **6,** 167.

[24] Goodby, J. W., Slaney, A. J., Booth, C. J., Nishiyama, I., Vuijk, J. D., Styring, P., and Toyne, K. J., 1994, *Mol. Cryst. liq. Cryst.*, **243,** 231.

[25] Wu, S.-L., Chen, D.-G., and Chen, S.-J., 1995, *Liq. Cryst.*, **264,** 39.

[26] Wu, S.-L., and Hsieh, W.-J., 1996, *Liq. Cryst.*, **6,** 783.